An experimental proposal for revealing contextuality in almost all qutrit states

Jayne Thompson,[1] Robert Pisarczyk,[1,2] Paweł Kurzyński,[1,3] and Dagomir Kaszlikowski[1,4,*]

[1] *Centre for Quantum Technologies, National University of Singapore, 3 Science Drive 2, 117543 Singapore, Singapore*
[2] *Department of Physics, University of Oxford, Oxford UK*
[3] *Faculty of Physics, Adam Mickiewicz University, Umultowska 85, 61-614 Poznań, Poland*
[4] *Department of Physics, National University of Singapore, 2 Science Drive 3, 117542 Singapore, Singapore*

Contextuality is a foundational phenomenon underlying key differences between quantum theory and classical realistic descriptions of the world. Here we propose an experimental test which is capable of revealing contextuality in all qutrit systems, except the completely mixed state, provided we choose the measurement basis appropriately. The experiment is based upon a recently derived result [Phys. Rev. A **86**, 042125]. The 3-level system is furnished by the polarization and spatial degrees of freedom of a single photon, which encompass three orthogonal modes. Projective measurements along rays in the 3-dimensional Hilbert space are made by linear optical elements and detectors which are sensitive to single mode. We also discuss the impact of detector inefficiency and losses.

PACS numbers: 03.65.Ta, 03.65.Ud

* phykd@nus.edu.sg

I. INTRODUCTION

In classical physics, all observable quantities have an objective reality. The outcome of measuring a classical observable A can not be influenced by a property of the observer or by the choice to simultaneously co-measured A with a second observable B. This property is referred to as non-contextual realism.

Distinctively, in quantum theories the measurement outcome for an observable A depends on what you choose to co-measure at the same time. There exist certain sets of observables where it is impossible to simultaneously assign pre-existing outcomes. In this scenario there is no joint probability distribution from which the measurement statistics for every observable can be recovered as marginals.

Recently Klyachko, Can, Binicioglu and Shumovsky introduced a 5-ray (KCBS) inequality [1]. The KCBS inequality uses the maximum attainable level of correlation between certain co-measurable observables belonging to any non-contextual realistic theory. By construction the KCBS inequality is satisfied by all non-contextual hidden variable models. However Klyachko et. al. discovered violation of the inequality in a 3-level quantum system. It has been shown that the KCBS inequality is the simplest possible test for contextuality of quantum theories, in the sense that any inequality based on projective measurements along less than five different direction will be satisfied by all classical and quantum theories [2]. The KCBS inequality formed the basis of several recent experimental tests of quantum contextuality. Lapkiewicz et. al. have experimentally demonstrated violation of the KCBS inequality in an indivisible 3-level quantum system (furnished by a single photon) [3]. This experiment built upon a robust and rapidly developing body of experimental continuality literature [4–9]. In our present work we draw on the tests outlined in these papers.

From the perspective of an experimental test of non-contextual realism the KCBS inequality is a state dependent test; for a sufficiently pure state there exists a choice of five measurement directions which can be used to detect violation of the KCBS inequality. Hence any experimental implementation requires a rigorous state preparation phase. For 3-dimensional systems there also exists a completely state independent test involving thirteen projectors developed by Oh and Yu [10] and an almost state independent test involving nine projectors [11]. The latter is capable of revealing contextuality in every state, except the maximally mixed state, provided we choose the measurement basis appropriately. We describe this inequality in more detail in Section III. It has been shown that thirteen rays is the minimum number of distinct projector directions necessary for a state independent test of non-contextual realism [12].

The purpose of this paper is to propose an experimental test for the inequality from Ref. [11]. The experimental set up will be along the lines of Lapkiewicz et al.'s KCBS inequality experiment [3]. We will also discuss the minimum detector efficiency required to ensure the results are independent of any auxiliary assumptions about photons in undetected events.

In Section II we discuss the key differences between non-contextual hidden variable theories which obey classical realism and quantum mechanics. We introduce the inequality and contextual results from Ref. [11] in Section III. In the following section we propose an experimental test of this inequality. We use Section V to analyze the effects of losses and detector inefficiency on this experiment. We conclude the paper with a brief summary of our results.

II. CONTEXTUALITY

Consider a theory with n observables, $A_1, \ldots A_n$, where each observable, A_i, returns outcome a_i with probability $p(A_i = a_i)$. This theory exhibits classical realism whenever there exists a joint probability distribution for the combined measurement outcomes $p(A_1 = a_1, \ldots, A_n = a_n)$ such that the measurement statistics, $p(A_i = a_i)$, of each observable, A_i, can be obtained as a marginal of this distribution [13]. In this scenario there exists a non-contextual hidden variable model, conditioned on a set of parameters Λ. The joint probability distribution is reproduced through

$$p(A_1 = a_1, \ldots, A_n = a_n) = \int d\lambda \; p(\lambda) p(A_1 = a_1|\lambda) \ldots p(A_n = a_n|\lambda), \tag{1}$$

where each strategy for assigning measurement outcomes, λ, has weighted probability $p(\lambda)$ on the set Λ, and $p(A_i = a_i|\lambda)$ is the conditional probability of obtaining an outcome a_i when measuring observable A_i (for the given non-contextual hidden variable λ).

Quantum theories do not necessarily exhibit non-contextual realism. When we measure an observable A_1 we simultaneously collapse the state we are observing onto an eigenstate of A_1. If A_1 is independently simultaneously co-measurable with either member of a non-commuting pair (A_2 and A_3), then choosing to measure A_1 simultaneously with A_2 (respectively A_3) can erase information about the correlations between A_1 and A_3 (respectively A_2). Because a joint measurement of A_1 and A_2 can erase different information from a joint measurement of A_1 and A_3, the two joint measurements do not need to be unitarily equivalent. The choice to simultaneously co-measure A_1 with either

A_2 or A_3 can influence the outcome of A_1. We say that these two non-commuting observables each furnish a context for A_1 and that quantum mechanics is a contextual theory.

Given a set of observables we can succinctly represent which subsets are compatible in a single graph. This graph has one vertex, v_i, for each observable A_i. The edge set of the graph is generated by connecting any two vertices v_i and v_j associated with compatible observables, respectively A_i and A_j, by an undirected edge (v_i, v_j).

III. A SPECIFIC TESTS OF CONTEXTUALITY

In this section we will explain a recently derived inequality from Ref. [11]. This inequality is based on nine projective measurements whose compatibility relations are provided by orthogonality and depicted in Figure 1. The nine vertices in Figure 1 can be identified with projective measurements $\Pi_i = |i\rangle\langle i|$, along the following nine rays in a 3-dimensional Hilbert space:

$$\begin{aligned}
|1\rangle &= (1,0,0),\\
|2\rangle &= (0,1,0),\\
|3\rangle &= (0,0,1),\\
|4\rangle &= 1/\sqrt{2}(0,1,-1),\\
|5\rangle &= 1/\sqrt{3}(1,0,-\sqrt{2}),\\
|6\rangle &= 1/\sqrt{3}(1,\sqrt{2},0),\\
|7\rangle &= 1/2(\sqrt{2},1,1),\\
|8\rangle &= 1/2(\sqrt{2},-1,-1),\\
|9\rangle &= 1/2(\sqrt{2},-1,1).
\end{aligned} \tag{2}$$

In a non-contextual theory, for any complete orthogonal basis[1] of rays $\{|u_i\rangle\}$ it is possible to assign values of 1 or 0 to the corresponding projectors Π_{u_i}, in such a way that $\Sigma_{u_i}\Pi_{u_i} = 1$ (completeness of the basis) and if a projector, Π_{u_i}, appears in two different complete basis then it is assigned the same consistent value in each basis (non-contextual condition) [14].

It follows that for any non-contextual realistic theory, where measurement statistics can be encapsulated in a hidden variable strategy $p(\lambda)$ as in (1), these nine-projectors satisfy:

$$\sum_{i=1}^{9}\langle\Pi_i\rangle \;\leq\; 3. \tag{3}$$

We can arrive at the contextuality inequality in Ref. [11], by replacing each of the projectors in Equation (3) by a dichotomous observable,

$$A_i = 1 - 2\Pi_i, \tag{4}$$

which assign values of $+1$ and -1 to measurement outcomes. In this notation Equation (3) becomes a statement about the correlations of observables $A_1, \ldots, A_9$ (in relation to the edge set $E(G)$ of Figure 1):

$$\sum_{(i,j)\in E(G)} \langle A_i A_j\rangle + \langle A_9\rangle \geq -4. \tag{5}$$

Given a quantum state ρ, which is not the maximally mixed state, it is possible to choose a basis for the 3-dimensional Hilbert space so that the inequality (3) will be violated. More explicitly, the state ρ violates Inequality (3) when you make projective measurements along the directions in Equation (2) relative to this basis [11]. Optimal violation will be obtained when we choose to measure with respect to the eigenbasis of ρ. To complement this analysis we have run a numerical simulation, using QI Mathematica package [15], which tested the inequality (3) for a prefixed measurement basis and a randomly generated sample of ten million density matrices weighted by the Hilbert-Schmidt measure. We found 49.98% of quantum states ρ violated (3).

---

[1] For the d-dimensional Hilbert space. The pertinent case being $d = 3$.

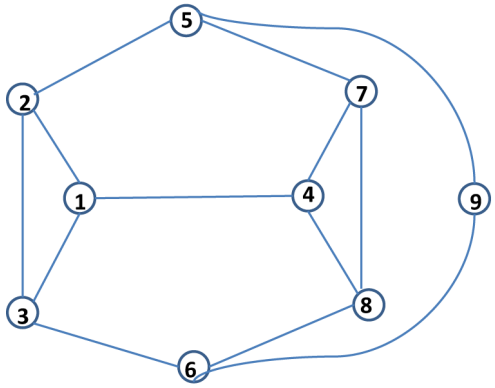

FIG. 1. The graph, G, of the orthogonality relations for the nine projectors in the inequality from Ref. [11].

For the purpose of the following experimental design it is pertinent that the projectors $|1\rangle$, $|2\rangle$ and $|3\rangle$ form a complete basis for the 3-dimensional Hilbert space. Hence for these projectors there is a completeness relation:

$$\langle A_1 A_2 \rangle + \langle A_2 A_3 \rangle + \langle A_3 A_1 \rangle = -1. \tag{6}$$

A similar relation holds for the complete basis $|7\rangle$, $|4\rangle$ and $|8\rangle$.

IV. EXPERIMENTAL DESIGN

Lapkiewicz et al. have experimentally demonstrated violation of the KCBS inequality for the indivisible 3-level quantum system furnished by a single photon [3]. A photonic qutrit uses two distinct spatial paths for the photon and within one of the spatial paths two optical modes propagate as distinct polarization modes. Here we propose a straightforward adaptation of Lapkiewicz et al.'s experiment to the inequality (5). The aim of our proposed experiment is to directly measure violation of the inequality (5) by a 3-level quantum system. This will involve taking simultaneous measurements of pairs of compatible observables A_i and A_j when the corresponding vertices v_i and v_j are connected by an edge in Figure 1. An implicit caveat on any experimental implementation of this proposal is that all experimental runs must be independent and the results after a statistically significant number of runs must represent an unbiased sampling from the joint probability distribution (1); in the case where the latter is tailored to the nine projective measurement constructed from (2). Later we will discuss how losses and detector inefficiencies may allow a joint probability distribution conditioned on a hidden variable to violate the inequality (5). In both scenarios we use a single photon heralded source which will alow us to monitor photon losses. Previous experiments, [3, 5], produce pairs of polarization entangled photons in the singlet state via parametric down conversion and subsequently rerouted one photon to an auxiliary detector 'detector 0'. Post selecting on whether this auxiliary detector clicks creates a heralded single photon, see Figure 3. Any desired initial state can be synthesized using polarizing beam splitters to combine the two spatial modes and half wave plates to transform the polarization components inside a single spatial mode.

We introduce a single detector for each mode (we will use the label: detector i, for $i = 1, 2$ or 3). Two scenarios are considered: in the first scenario there are no losses and detector i will click whenever a photon is in the corresponding mode $|i\rangle$. In the second scenario we will allow for inefficient detectors. We revisit this scenario later. It is convenient to identify the three orthogonal modes with rays $|1\rangle, |2\rangle$ and $|3\rangle$ from Equation (2). If detector i clicks then we record $\Pi_i = 1$ and using Equation (4) we assign a value $A_i = -1$ to the corresponding dichotomous observable.

The correlations of two dichotomous observables are given by:

$$\begin{aligned}\langle A_i A_j \rangle &= P(A_i = A_j = 1) + P(A_i = A_j = -1) - P(A_i = 1, A_j = -1) - P(A_i = -1, A_j = 1) \\ &= 1 - 2P(A_i = 1, A_j = -1) - 2P(A_i = -1, A_j = 1).\end{aligned} \tag{7}$$

The second line follows because (with unit probability) either both A_i and A_j are equal to 1, alternatively both are equal to -1, or precisely one of them is equal to -1. We only count results from experimental runs where a single detector clicks coincidentally with detector 0. This implies that in all events contributing to Equation (7) the sum of the measurement outcomes for the dichotomous observables (during a single run) is equal to -1 (in the first instance $A_1 + A_2 + A_3 = -1$). Furthermore when A_i and A_j correspond to orthogonal modes we discount experimental runs where $A_i = A_j = -1$ causing $P(A_i = A_j = -1) = 0$.

Repeated runs of this experimental configuration can be used to measure the correlations $\langle A_1 A_2 \rangle$, $\langle A_1 A_3 \rangle$ and $\langle A_2 A_3 \rangle$. A full experiment capable of measuring all the correlation in the inequality (5) can be obtained by adding standard optical elements; specifically half wave plates and polarizing beam splitters. If we pass the input modes $|1\rangle$, $|2\rangle$ and $|3\rangle$ through a series of half wave plates and polarizing beam splitters then we can output the orthogonal modes for any three rays $|i\rangle, |j\rangle$ and $|k\rangle$ which are a linear combination of $|1\rangle, |2\rangle$ and $|3\rangle$, and form a basis for the 3-dimensional Hilbert space. At every stage of the experiment each detector is aligned to detect photons in a single mode. It is assumed that this detector will click if the photon is in the corresponding mode.

A schematic of the sequence of optical elements and measurements needed to obtain all the correlations in the inequality (5) is depicted in Figure 2. The physical implementation of this experiment will require exact details regarding the sequence of half wave plates and polarizing beam splitters needed to appropriately mix the two different polarization modes within a single spatial mode and subsequently mix the spatial modes. We leave the nuances of the setup to the discretion of an experimental group. In Figure 3 we give a proof of principle that the schematic given in Figure 2 is physically realizable using an adaptation of Lapkiewicz et al.'s design [3]. For more detail see Appendix A which contains Figure 3 and lists the transformations enacted by the half wave plates.

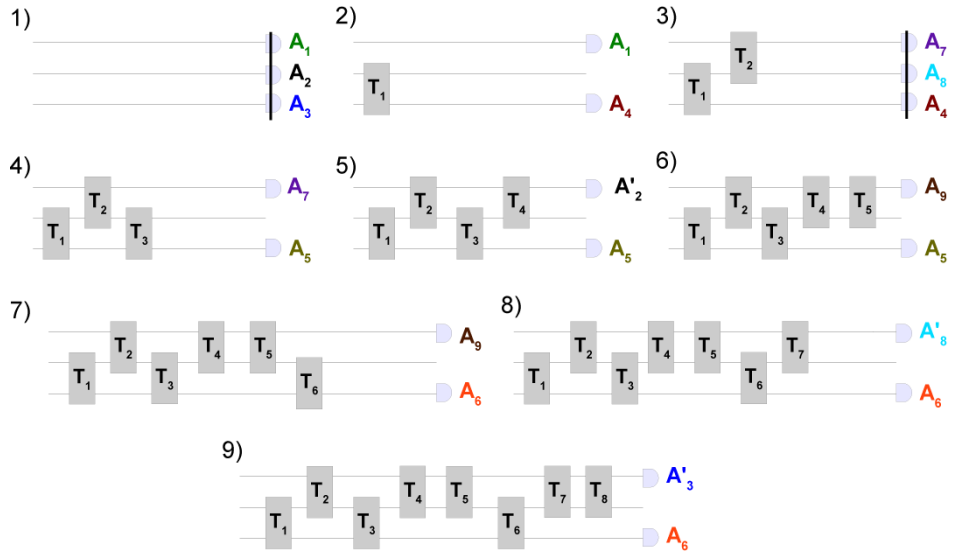

FIG. 2. Each subfigure represents an experimental configuration which measures $\langle A_i A_j \rangle$ for the specific A_i and A_j indicated on the righthand side of the subfigure. Orthogonal modes are represented by horizontal lines. Sequences of half wave plates and polarizing beam splitters are labeled $T_1, \ldots, T_8$ and detector positions are indicated by the corresponding dichotomous observable. The expectation value $\langle A_9 \rangle$ can be obtained from the data collected during the experimental runs depicted in subfigures 6) or 7). The vertical line through the detectors in subfigures 1) and 3) indicate it is not necessary to record data during these stages. This follows from Equation (6). The precise sequence of optical elements $T_1, \ldots, T_8$ are recorded in Figure 3 which should be read in conjunction Table A in Appendix A. In this schematic when two consecutive stages of the experiment involve measuring the same mode, $|i\rangle$, and the beam line of mode $|i\rangle$ is unobstructed between the points at which these two measurements are made, we assume the physical implementation will measure the (same) mode $|i\rangle$ in two different contexts. The difference between A_2 in subfigure 1) and A_2' in subfigure 5) is explained in detail in Section IV.

It is implicitly assumed that at any stage of the experiment; if a given mode's beam line is not interrupted by an optical element then there is perfect transmission of any photon (amplitude component) in this mode. This occurs regardless of whether the other two modes pass through a half wave plate or are obstructed.

Notice that according to Figure 2, we first measure the mutual correlations of the dichotomous observables, A_1, A_2, A_3, corresponding to orthogonal modes $|1\rangle$, $|2\rangle$ and $|3\rangle$. Subsequently in subfigure 5) we need to measure $\langle A_2 A_5 \rangle$, however during the intermediary stages the beam line of mode $|2\rangle$ has been interrupted. This introduces a source of error. We must recreate the mode $|2\rangle$ before measuring $\langle A_2 A_5 \rangle$. We can not be certain that in both instances we are measuring the precisely the same orthogonal mode $|2\rangle$. To accommodate this we distinguish between the observable A_2 in subfigure 1) and the observable A_2' measured in subfigure 5) of Figure 2. We correspondingly

modify the inequality to

$$\sum_{(i,j)\in E(G)} [\langle A_i A_j\rangle(1-\delta_{i5}\delta_{j2}-\delta_{i,6}\delta_{j8}-\delta_{i6}\delta_{j3})] + \langle A_5 A_2'\rangle + \langle A_6 A_8'\rangle + \langle A_6 A_3'\rangle + \langle A_9\rangle \geq -1-\epsilon_a-\epsilon_b-\epsilon_c, \quad (8)$$

by including the error terms $\epsilon_a = 1-\langle A_2 A_2'\rangle,\ \epsilon_b = 1-\langle A_8 A_8'\rangle,\ \epsilon_c = 1-\langle A_3 A_3'\rangle$.

In principle the method for obtaining each error terms is identical and is outlined in Ref. [3]. Therefore without loss of generality we explicitly focus on measuring the error term $\epsilon_a = \langle A_2 A_2'\rangle$. We can obtain ϵ_a directly by using Equation (7) to determine the value of $\langle A_2 A_2'\rangle$. It is not possible to measure modes $|2\rangle$ and $|2'\rangle$ concurrently. However we conclude from Equation (7) that:

$$\epsilon_a = 2P(A_2 = 1, A_2' = -1) + 2P(A_2 = -1, A_2' = 1). \quad (9)$$

To find the above probabilities we set up the experiment with the intention of measuring A_2' but place a card[2] at the point where mode $|2\rangle$ is first created. This card should effectively block photons belonging to second orthogonal mode in subfigure 1) of Figure 2. This will exclude all events where $A_2 = -1$. If the detector measuring A_2' clicks then we record an event where $A_2 = 1$ and $A_2' = -1$. This will allow us to find $P(A_2 = 1, A_2' = -1)$. We can chose to unblock mode $|2\rangle$ and instead block the other two modes: $|1\rangle$ and $|3\rangle$ in Figure 2. In this scenario we exclude all events where $A_2 = 1$. When the detector measuring A_2' does not click we have an event where $A_2 = -1$ and $A_2' = 1$. This will allow us to find $P(A_2 = -1, A_2' = 1)$.

Finally we highlight that Equation (6) implies we do not need to collect data during the experimental stages depicted in subfigures 1) and 3) of Figure 2. We have drawn a vertical line through the detectors whenever it is not necessary to collect data. We include these stages in the schematic because it is important to comprehensively set up all the measurement configurations. We need to ensure the orthogonal modes have the same relative orientations (and orthogonality relations) as the projectors in Equation (2). This makes it essential to setup all stages of the experiment.

Errors will arise from imperfect alignment of half wave plates. This will cause some of the modes to be be misaligned with the rays in Equation (2). In this case we will be testing the inequality (5) using projective measurement along directions which do not perfectly match the list in Equation (2). The nine direction in Equation (2) corresponded to a theoretically optimal set of projective measurements for testing the inequality (5). The errors introduced by half wave plate misalignment will make it more difficult to experimentally violate this inequality. However they will not invalidate any experimental results which directly demonstrate violation.

We now come back to the second scenario: in any realistic experiment there will be runs where the photon is lost and none of the detectors click. These losses are caused by reflections off half wave plates and detector inefficiencies. To ensure the results will not be biased by losses we only consider data from experimental runs where a single detector clicks. This approach requires the subsidiary assumption that for all runs the probability of loosing a photon is not correlated with the measurement outcome. In the next section we consider how efficient the experiment must be in order to eliminate this assumption.

V. DETECTION LOOP HOLE

Without loss of generality we can assume all photons are lost at the detector. We attribute an efficiency η to each of the three detectors. We want to make our results independent of the distribution of photon modes in undetected runs. To do this we include the runs where none of the detectors click. The combined total number of runs is constituted by runs where either a single detector clicks or none of the detectors click.

In the ideal scenario where there are no losses, $p(A_i = a_i)$ is the probability of getting outcome a_i when you measure observable A_i. When we include losses we use $p'(A_i = a_i) = \eta p(A_i = a_i)$ for the proportion of the combined total number of runs where we measure A_i and get outcome a_i.

To uniquely specify the results of a run we must specify the outcomes a_i, a_j and a_k of all three dichotomous observables (respectively A_i, A_j and A_k).

When estimating the correlations in Equation (7) we now use the renormalized probability:

$$\widetilde{p}(A_i = a_i, A_j = a_j, A_k = a_k) = \frac{p'(A_i = a_i, A_j = a_j, A_k = a_k)}{1 - p'(A_i = A_j = A_k = 1)}, \quad (10)$$

[2] A practical implementation of this experiment uses only two spatial modes. At each stage of the experiment two of the levels (in the three level system) will have the same spatial mode index (but opposite polarization indices). Therefore the practical implementation of this scheme may require the card to be opaque only to photons in the polarization mode associated with $|2\rangle$.

which is the ratio of the number of runs with the given outcome $(A_i = a_i, A_j = a_j, A_k = a_k)$ to the number of runs where a single detector clicks. This eliminates the dependence on no detection events (runs with outcome $A_i = A_j = A_k = 1$).

In hidden variable theories we can use (1) to express $\widetilde{p}(A_i = a_i, A_j = a_j, A_k = a_k)$ as a function of the detector efficiency η and probabilities in the ideal scenario where there are no losses:

$$\widetilde{p}(A_i = a_i, A_j = a_j, A_k = a_k) = \frac{1}{1-(1-\eta)} \int d\lambda \; p(\lambda) \; \eta p(A_i = a_i|\lambda) \; \eta p(A_j = a_j|\lambda) \; \eta p(A_k = a_k|\lambda). \tag{11}$$

This allows us to evaluate the correlations in Equation (7) for a hidden variable strategy $p(\lambda)$ conditioned on λ. We find the inequality (5) is modified in the presence of detector inefficiency to

$$\sum_{(i,j)\in E(G)} \langle A_i A_j \rangle + \langle A_9 \rangle \geq -4/\eta^2. \tag{12}$$

We need $\eta > 0.82$ for the right hand side of Equation (12) to be below the maximum level of quantum violation for this inequality [16]. Hence when the detector efficiency is below 82% it is impossible to experimentally detect violation of the inequality (5) unless subsidiary assumptions are made about the distribution of putative outcomes (which detector failed to click) for undetected events.

VI. CONCLUSION

In conclusion we propose an experimental test of the inequality from Ref. [11]. An experimental implementation would test one of the foundational principles which distinguish quantum mechanics from classical realistic descriptions of the world. Furthermore if this test reveals contextual behavior in an indivisible spin one system then the behavior can not stem from entanglement. This result complements work done on the KCBS inequality [1, 3] as well as the thirteen projector state independent inequality from Ref. [5, 10]. We present numerical studies which indicate the inequality (5) is violated by 49.98% of states in a 3-level system. This makes an experimental test less sensitive to state preparation.

ACKNOWLEDGMENTS

This work was supported by the National Research Foundation and Ministry of Education in Singapore. PK is also supported by the Foundation for Polish Science. We thank Valerio Scarani and Rafael Rabelo for useful discussions on the experimental set up. JT thanks Mile Gu for insight into the correlations of exclusive observables. RP thanks Dagomir Kaszlikowski and Centre for Quantum Technologies for hosting his visit to Singapore and nurturing his budding film career.

Appendix A: Half wave plate orientations

This appendix contains details of a possible implementation of Schematic 2.

The table lists the transformations that half wave plates $WP1 - WP6$ enact on the two polarization modes. Each angle corresponds to the angle of rotation in a 2×2 rotation matrix acting on a pair of polarization modes within a single spatial path. We have chosen to give the angle characterizing the transformation rather than the precise configuration of the wave plate's optical axis because the latter will be contingent on the exact details of the experimental implementation and may be obsolete if even a small change is made. The '$-$' indicates that the corresponding wave plate is unnecessary for measuring the corresponding correlation.

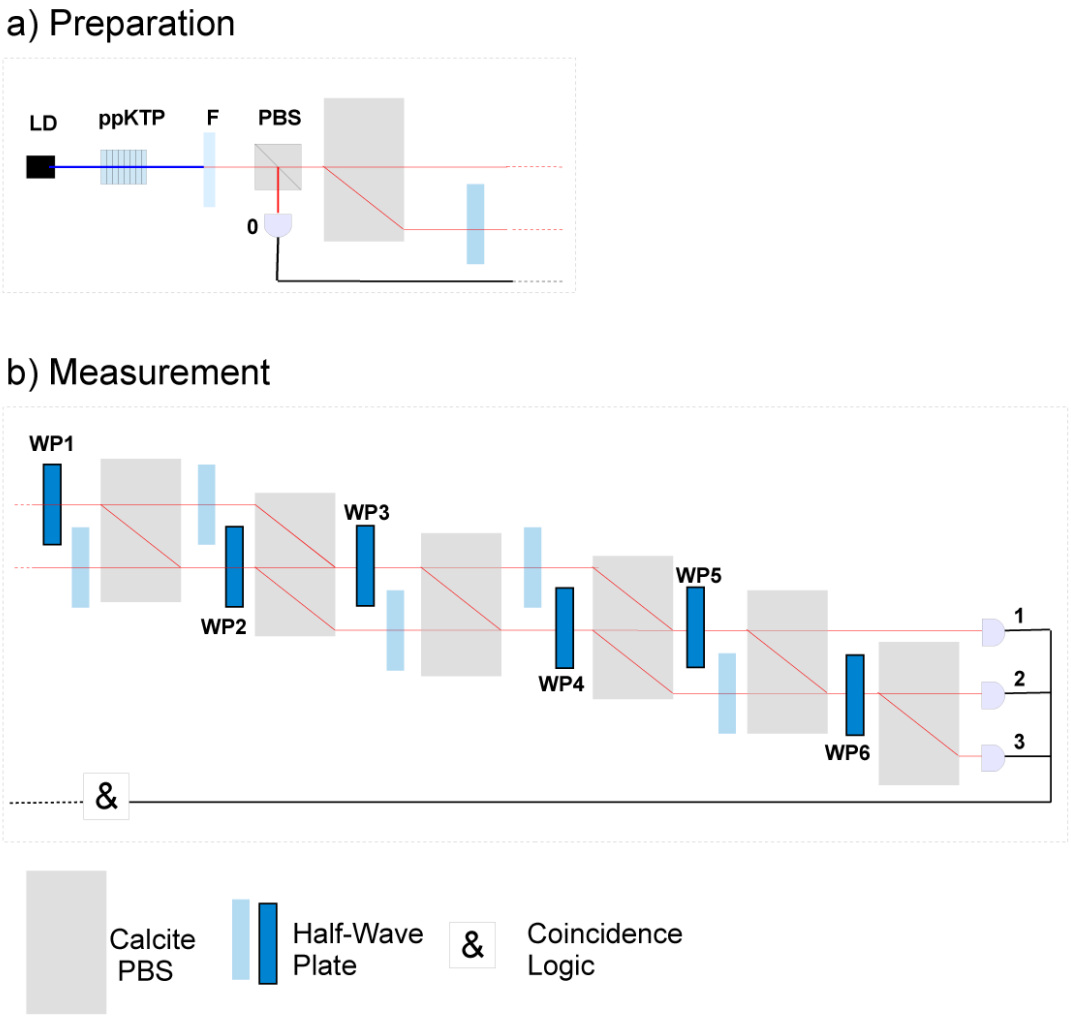

FIG. 3. Here we give a possible experimental implementation of Schematic 2 in the spirit of Lapkiewicz et. al. [3]. **Preparation**: a single photon heralded source is created through parametric down conversion; a process which outputs pairs of polarization entangled photons in the singlet state. Subsequently a polarizing beam splitter is used to redirect one member of the pair to a heralding detector: 'detector 0' which is denoted by '**0**' in the figure. Post selecting on events where detector 0 clicks clearly identifies runs where the photon is lost (detector 0 is the only detector to click) as distinct from runs where the photon is not lost (one of detectors 1-3 click coincidentally with detector 0). We take inspiration from Ref. [3] which used a 405 nm Laser diode (LD) in combination with a nonlinear-periodically-poled-Potassium-Titanyl-Phosphate-crystal (ppKTP) and suitable filters (F) to produce pairs of polarization entangled photons. For a comprehensive explanation of this process see Ref. [3]. Any desired initial state can now be synthesized using additional half wave plates and polarizing beam splitters. **Measurement**: there are always two concurrent modes with the same spatial index and opposite (orthogonal) polarization indices. Half wave plates $WP1 - WP6$ manipulate these two modes. Each wave plate implements a 2×2 rotation on the two dimensional subspace spanned by the pair of polarization modes within a single spatial path. The angles characterizing these rotations are given in Table A. Modes with different spatial indices can be recombined using polarizing beam splitters which are represented by grey rectangles. We use 0 radians to denote the configuration of an optical element (alignment of the optical axis) which implements the identity transformation. The remaining light-blue wave plates have been inserted to balance the path lengths of the two spatial modes; these are all set to $\pi/4$ (this alignment balances a π phase shift between the two spatial modes). When the run requires a subset of the optical elements, the unnecessary elements can be aligned to identity transformations. Note that in Figure 2 transformations T_4 and T_5 act consecutively on the same two-mode subspace. In the physical implementation T_4 and T_5 correspond to wave plate $WP4$ set to two different orientations, see Table A. Analogously T_7 and T_8 use two different settings of $WP6$.

Correlations measured	$WP1$	$WP2$	$WP3$	$WP4$	$WP5$	$WP6$
$\langle A_1 A_2\rangle$ $\langle A_1 A_3\rangle$ $\langle A_2 A_3\rangle$	-	-	-	-	-	-
$\langle A_1 A_4\rangle$	$\frac{3\pi}{4}$	-	-	-	-	-
$\langle A_7 A_8\rangle$ $\langle A_8 A_4\rangle$ $\langle A_7 A_4\rangle$	$\frac{3\pi}{4}$	$\frac{\pi}{4}$	-	-	-	-
$\langle A_5 A_7\rangle$	$\frac{3\pi}{4}$	$\frac{\pi}{4}$	$\cos^{-1}(\frac{1}{\sqrt{3}})$	-	-	-
$\langle A'_2 A_5\rangle$	$\frac{3\pi}{4}$	$\frac{\pi}{4}$	$\cos^{-1}(\frac{1}{\sqrt{3}})$	$\frac{\pi}{3}$	-	-
$\langle A_9 A_5\rangle$	$\frac{3\pi}{4}$	$\frac{\pi}{4}$	$\cos^{-1}(\frac{1}{\sqrt{3}})$	$\frac{13\pi}{12}$	-	-
$\langle A_9 A_6\rangle$	$\frac{3\pi}{4}$	$\frac{\pi}{4}$	$\cos^{-1}(\frac{1}{\sqrt{3}})$	$\frac{13\pi}{12}$	$\cos^{-1}(\frac{1}{3})$	-
$\langle A'_8 A_6\rangle$	$\frac{3\pi}{4}$	$\frac{\pi}{4}$	$\cos^{-1}(\frac{1}{\sqrt{3}})$	$\frac{13\pi}{12}$	$\cos^{-1}(\frac{1}{3})$	$-\frac{\pi}{3}$
$\langle A'_3 A_6\rangle$	$\frac{3\pi}{4}$	$\frac{\pi}{4}$	$\cos^{-1}(\frac{1}{\sqrt{3}})$	$\frac{13\pi}{12}$	$\cos^{-1}(\frac{1}{3})$	$\frac{\pi}{3}$

[1] A. A. Klyachko, M. A. Can, S. Binicioglu, and A. S. Shumovsky, Phys. Rev. Lett. **101**, 020403 (2008).
[2] Kurzynski, Ramanathan, Kaszlikowski, Phys. Rev. Lett. **109**, 020404 (2012) arXiv:1201.2865
[3] R. Lapkiewicz, P. Li, C. Schaeff, N. K. Langford, S. Ramelow, M. Wieniak, and A. Zeilinger, Nature (London) **474**, 490 (2011).
[4] G. Kirchmair, F. Zhringer, R. Gerritsma, M. Kleinmann1, O. Ghne, A. Cabello, R. Blatt, and C. F. Roos, Nature **460**, 494-497 (2009)
[5] C. Zu, Y.-X. Wang, D.-L. Deng, X.-Y. Chang, K. Liu, P.-Y. Hou, H.-X. Yang, and L.-M. Duan Phys. Rev. Lett. **109**, 150401 (2012)
[6] O. Moussa, C. A. Ryan, D. G. Cory, and R. Laflamme Phys. Rev. Lett. **104**, 160501 (2010)
[7] H. Bartosik, J. Klepp, C. Schmitzer, S. Sponar, A. Cabello, H. Rauch, and Y. Hasegawa Phys. Rev. Lett. **103**, 040403 (2009)
[8] E. Amselem, L. E. Danielsen, A. J. Lopez-Tarrida, J. R. Portillo, M. Bourennane, and A. Cabello Phys. Rev. Lett. **108**, 200405 (2012)
[9] A. Cabello, Phys. Rev. A **85**, 032108 (2012)
[10] S. Yu, C. H. Oh, Phys. Rev. Lett. **108**, 030402 (2012)
[11] P. Kurzynski, D. Kaszlikowski, Phys. Rev. A **86**, 042125 (2012) arXiv:1207.1212
[12] A. Cabello, eprint arXiv:1201.0374
[13] A. Fine, Phys. Rev. Lett. **48**, 291 (1982).
[14] A. Peres, J. Phys. A: Math. Gen. **24** L175 (1991)
[15] J.A. Miszczak, Int. J. Mod. Phys. C, **22**, 897-918 (2011)
[16] B.S. Cirel'son, Letters in Mathematical Physics **4**, 93-100 (1980).